Published in final edited form as:
Arch Oral Biol. 2011 April ; 56(4): 331–336. doi:10.1016/j.archoralbio.2010.10.017.

Altered self-assembly and apatite binding of amelogenin induced by N-terminal proline mutation

Li Zhu[a,*], **Vuk Uskoković**[b,*], **Thuan Le**[a], **Pamela DenBesten**[a], **Yulei Huang**[a,c], **Stefan Habelitz**[b], and **Wu Li**[a,**]

[a]Department of Orofacial Sciences, School of Dentistry, University of California, San Francisco, CA94143, United States

[b]Department of Preventive & Restorative Dental Sciences, School of Dentistry, University of California, San Francisco, CA94143, United States

[c]Department of Oral Medicine, Guanghua School of Stomatology, Sun Yat-sen University, Guangdong, PR China

Abstract

Objective—A single Pro-70 to Thr (p.P70T) mutation of amelogenin is known to result in hypomineralized amelogenesis imperfecta (AI). This study aims to test the hypothesis that the given mutation affects the self-assembly of amelogenin molecules and impairs their ability to conduct the growth of apatite crystals.

Design—Recombinant human full-length wild-type (rh174) and p.P70T mutated amelogenins were analyzed using dynamic light scattering (DLS), protein quantification assay and atomic force microscopy (AFM) before and after the binding of amelogenins to hydroxyapatite crystals. The crystal growth modulated by both amelogenins in a dynamic titration system was observed using AFM.

Results—As compared to rh174 amelogenin, p.P70T mutant displayed significantly increased sizes of the assemblies, higher binding affinity to apatite, and decreased crystal height.

Conclusions—Pro-70 plays an important structural role in the biologically relevant amelogenin self-assembly. The disturbed regularity of amelogenin nanospheres by this single mutation resulted in an increased binding to apatite and inhibited crystal growth.

Keywords

amelogenin; tooth enamel; hydroxyapatites; biomineralization; self-assembly

1. Introduction

Amelogenesis imperfecta (AI) is a group of genetically transmitted enamel defects[1,2]. Mutational analysis of families with X-linked hypomaturation AI revealed a substitution of

**Corresponding author: Wu Li, Department of Orofacial Sciences, University of California, San Francisco, 513 Parnassus Avenue, San Francisco, CA 94143, USA, Wu.Li@ucsf.edu Phone: +1-415-476-1037 Fax: +1-415-476-4204 .
*Equally contributed as first authors

adenine for cytosine in exon 6 of the amelogenin gene that results in a proline to threonine change at position 70 (p.P70T) in the protein[3]. The affected enamel exhibits less mineral and a higher protein content as compared to normal enamel[3-5]. Amelogenins are proline-rich proteins that constitute the predominant component in the mineralizing enamel matrix. Pro-70 is highly conserved in amelogenin among many identified species and is in close proximity to a normal amelogenin cleavage site. Our previous *in vitro* studies verified that the p.P70T substitution caused a delay in the proteolytic cleavage of amelogenin by MMP20[6]. The high conservation and particular location of this proline imply its important functional roles. Despite extensive studies, the mechanism by which the p.P70T mutation of amelogenin distorts the normal enamel formation and hence contributes to the pathogenesis of AI is still unclear.

Amelogenin undergoes a spontaneous assembly to form nanospheres that are presumed as the basic building blocks for the initiation and oriented elongation of enamel crystals[7]. The assembly is driven by hydrophobic interactions and affected by pH, temperature and protein concentration[8,9]. The tightly associated amelogenin nanospheres interact with apatite crystals, adhering thereto and protecting them from premature fusion[10]. Research has shown that the lack of the hydrophilic C-terminus of amelogenin caused a reduction in the binding affinity to apatite and an interruption of amelogenin self-association[8,11]. During the enamel development, amelogenin proteins are progressively processed and eventually removed from the extracellular space to allow the mineral crystals to grow[12]. The AI-like phenotype observed in amelogenin knockout mice provides further strong evidence for the essential role of amelogenin in the modulation of enamel crystal growth[13].

We hypothesize that the p.P70T point mutation affects the proper amelogenin-amelogenin and amelogenin-mineral interactions, which results in inhibited enamel crystal growth. These results, together with other basic studies, will provide a deeper insight into the pathological basis of AI, and also advance our understanding of the functions of proline residues in amelogenin. In that respect, the purpose of this paper is dual; on one hand, it serves the purpose of enabling us to grasp a deeper understanding of the bases of AI on the molecular level, whereas on the other hand it aims at elucidating the extent to which a single point mutation, in this case p.P70T, can affect a self-assembly of amelogenin and its interaction with the mineral phase.

2. Materials and methods

2.1. Apatite and protein preparation

Carbonated hydroxyapatite (CHAP) was synthesized as previously described[14-16], and characterized by X-ray diffraction[16]. Apatite powders were sequentially passed through 30 and 60 μm meshes and only particles with sizes between 30 and 60 μm were collected for the experiments undertaken in this study. The specific surface area of the apatite powder was 74.7 m^2/g[16].

Recombinant human full-length amelogenin wild-type (rh174) and the mutant with Pro-70 to Thr mutation (p.P70T) were expressed in *E. coli*, purified and identified as described previously[17,18] .

2.2. Dynamic light scattering (DLS) study of assembly

DLS analysis of rh174 amelogenin and p.P70T mutant was carried out using a DynaPro MS/X molecular sizing instrument equipped with a MicroSampler (ProteinSolutions Inc., Charlottesville, VA,). Thirty μl of amelogenin (0.5 mg/ml) in 20 mM Tris-HCl buffer was injected into a quartz cell. Tris-HCl was previously adjusted to pH 7.4 at different temperatures to achieve the desired pH value at a given temperature. After inserting the

quartz cell into the temperature-controlled chamber, samples were equilibrated for 10 min at 25 °C or 37 °C before DLS data were collected. Approximately 20 DLS measurements were obtained for each sample to provide adequate data replicates.

2.3. Atomic force microscopy (AFM) detection of amelogenin assemblies on apatite

The glass-ceramic used in this study contained rod-shaped fluoroapatite (FAP) crystals embedded in silica matrix[9,19-21]. This glass-ceramic is unique due to the uniaxial alignment of apatite crystals obtained by high-temperature extrusion processing[19]. Prior to the crystal growth experiments, the glass-ceramic substrates were sectioned and polished to expose the predominant (001) plane of the extruded FAP rods. Each substrate was placed in a prelubricated microcentrifuge tube (Corning, Inc., Corning, NY) containing rh174 at concentration of 0.5 mg/ml (pH 7.4). After incubation with mild shaking for 60 min at 25°C, the substrates were rinsed with a few drops of deionized water and immediately dried with canned air. The microstructure of proteins immobilized onto the substrates was observed using Nanoscope III AFM (Digital Instruments, Santa Barbara, CA). Images were obtained in dry conditions using the tapping mode with high aspect-ratio Si-tips (r ~ 5 nm, I ~ 125 μm) (Nanosensors, Neuchatel, Switzerland) operating at approximately 300 kHz[22].

2.3. Protein assays of amelogenin binding affinity

CHAP (0.5 mg) was thoroughly equilibrated in binding buffer (20 mM Tris-HCl, pH 7.4) in prelubricated tubes. To determine the maximum adsorption amount, different quantities of rh174 and p.P70T amelogenins (20, 40, 60, 80, 100, 120, and 140 μg) were incubated with the equilibrated CHAP for 60 min at room temperature on a shaking incubator. After centrifugation at 5,000 g for 5 min, the unbound proteins remaining in the supernatant were quantified by Bradford assay (BioRad, Hercules, CA, USA). The time curves for binding of these two amelogenins were obtained by incubating 150 μg protein with 0.5 mg CHAP and collecting samples at different time points from 0 to 60 min. Experiments were performed in triplicate and statistical differences were calculated by Student'+s *t* test in Prism software (GraphPad Software, Inc., La Jolla, CA, USA). Both the proteins remaining in supernatant and bound on CHAP were also subjected to SDS-PAGE analysis.

2.4. Amelogenin-guided apatite growth

To study the effects of rH174 and p.P70T on apatite growth, dynamic precipitation experiments were carried out[23]. The polished FAP-glass ceramic substrates were immersed in 0.4 mg/ml protein suspended in 20 mM Tris/HCl (pH 7.40), 150 mM KCl, 0.2% NaN_3 and 2.5 mM KH_2PO_4. Two titrants comprising: a) 8.2 mM $CaCl_2$, 284 mM KCl and 20 mM Tris/HCl (pH 7.40 ± 0.02), and b) 5 mM KH_2PO_4, 7 mM KOH, and 20 mM Tris/HCl (pH 7.40 ± 0.02), were subsequently introduced into the reaction system in parallel at the constant rate of 1.2 ml/day at 37 °C, cumulatively, throughout the 7-day period of time. A single substrate was sampled out each day and evaluated for the crystal growth properties using Atomic Force Microscopy (AFM, *Nanoscope III, Digital Instruments*). The crystal heights were measured using the section analysis tool in NanoScope software. Heights of twelve randomly chosen peaks in three different 10 × 10 μm AFM images were measured and the average values were plotted as a function of the reaction time. Tapping-mode AFM was applied using Si-tips with a radius of about 5 nm (*Supersharp, Nanosensors, Neuchatel, Switzerland*).

3. Results

3.1 Effects of p.P70T mutation on amelogenin assembly detected by DLS

The average hydrodynamic radii (R_h) and polydispersity values (Cp) of rh174 and p.P70T amelogenins at concentration of 0.5 mg/ml were measured by DLS analysis. At 25 °C, the average particle size formed by wild-type rh174 amelogenin was found to be 21.7 ± 0.8 nm with Cp value of 22.0%. Upon an increase in temperature to 37 °C, the nanospheres appear to be slightly larger (R_h = 25.9 ± 2.7 nm) and more heterogeneous (Cp=34.2%). In marked contrast, the p.P70T mutant formed significantly larger nanospheres with much wider size distribution at both temperatures (39.5 ± 3.0 nm with Cp value of 41.7 % at 25 °C, and 75.8 ± 9.6 nm with Cp value of 50.4% at 37 °C, $P < 0.01$ for both), indicating that the p.P70T mutation altered the sizes of the assemblies, especially at higher temperatures.

3.2. Comparison of rh174 and p.P70T amelogenin assemblies adhered to apatite surface by AFM

AFM measurements showed that the assembled proteins, either rh174 or p.P70T, were able to bind to the surfaces of both glass (darker area) and FAP crystals (lighter area) at their 001 faces (Fig. 1A and 1B). The nanospheres of rh174 deposited on the FAP surface were observed to possess uniform sizes between 20 and 30 nm (Fig. 1C). Consistent with the DLS observation, the nanospheres of p.P70T mutant were generally larger (30-60 nm) (Fig. 1D). In addition, some even larger (> 60 nm) as well as smaller nanospheres (< 15 nm) of p.P70T mutant were found on both crystal and glass surfaces (Fig. 1B and 1D), suggesting that its assemblies were relatively more polydisperse than those formed by rh174 amelogenin (Fig. 1A and 1C).

3.3. Comparisons of apatite-binding affinity between rh174 and p.P70T amelogenins

After incubation with the apatite crystals, the amounts of the adsorbed amelogenins were quantified. As shown in Fig. 2A and 2B, p.P70T amelogenin displayed much higher binding affinity as compared to rh174, though both of them quickly reached their adsorption saturation after 30-minute incubation. The saturated binding amount of rh174 amelogenin and p.P70T mutant were 875 ± 37 and 1194 ± 32 $\mu g/m^2$, respectively. Data analysis using Student's *t* test showed a significant difference between these two groups ($P < 0.01$). The SDS-PAGE results further confirmed that more of the mutated amelogenin was bound to the apatite (lane 6), leaving less protein remaining in supernatants (lane 4) (Fig 2C).

3.4. Effects of p.P70T and rh174 on the growth of apatite

Fig. 3A and 3B shows the morphology of the FAP crystals obtained in the dynamic precipitation experiments after 4.2 ml of the titration volume. Whereas there was no significant growth observed for the crystals immersed in p.P70T solution (Fig.3C), samples analyzed after the same reaction time in rh174 were covered with crystals grown up to 700 ± 100 nm in height (Fig.3B). Fig.3C demonstrates that the crystal growth is delayed in the presence of p.P70T as well as that the final crystal height, at the end of the 7-day experiment, is significantly lower in the mutant-comprising system.

4. Discussion

Our previous research revealed that the p.P70T mutation in amelogenin significantly decelerated amelogenin degradation by matrix metalloproteinase 20 (MMP20), highlighting the importance of this proline in amelogenin-MMP20 interactions[6,18,24]. In the present study, we further found that this specific mutation also affected the self-assembly and adsorption behavior of amelogenin, resulting in significantly inhibited crystal growth.

Conformational analyses suggest that amelogenin undergoes considerable structural transition from PPII/unordered conformation to ordered β-sheet upon self-assembly[25], supporting the idea that amelogenin self-assembly is contingent on the intrinsic propensities of the polypeptide chain. As shown by our DLS measurements, the sizes of amelogenin aggregates after the p.P70T mutation doubled at 25 °C and tripled at 37 °C, which along with the increased polydispersity indicates an impaired self-assembly process. These findings are broadly consistent with the previous research on recombinant histidine-tagged murine amelogenins (R_h of 20.7 ± 2.9 nm for wild-type and 45.5 ± 9.0 for p.P70T mutation at 25°C) [26]. Our subsequent AFM analysis provided further evidence that the p.P70T mutation influenced the extent and nature of amelogenin assembly, resulting in the formation of larger assemblies on apatite crystals. The dramatic differences observed between these two protein nanospheres suggested that the p.P70T alteration did affect amelogenin-amelogenin interactions during the self-assembly, which raises a question of how a single amino acid substitution can cause such substantial changes. This may be attributable to the unique characteristics of proline residue, the only amino acid containing a pyrrolidine five-member ring that reduces the structural flexibility of the peptide backbone. Proline often acts as potent breaker of β-sheet and frequently induces the reverse turn of β-hairpin in proteins[27]. Proline is commonly found in the edge strands in β sheets, presumably to avoid the “edge-to-edge” association between proteins that may lead to uncontrolled aggregation. It has been previously observed that substitution of proline residues results in an increased susceptibility of the protein to aggregation at elevated temperatures[28]. Pro-70 of amelogenin is located at the end of self-assembly domain A that is shown to be β-sheet dominant and essential for direct protein-protein interactions[26]. The replacement of this proline with threonine that lacks a β-carbon and has more back conformational flexibility may facilitate the extension of β-strand on the edge of β-sheet in the A domain, increasing the potential for edge-to-edge aggregation. As a result, larger and more heterogeneous nanospheres are formed, as observed by DLS and AFM in our present study.

Amelogenin molecules assemble into nanospheres by means of binding at the hydrophilic regions in the N- and C-terminus[29]. The hydrophobic central region of amelogenin forms a dense core of the nanospheres surrounded by extended C-terminal tail and slightly buried N-terminus[29,30]. Although the highly charged C-terminus of amelogenin has significant apatite binding affinity, the pretreatment of CHAP apatite with C-terminal telopeptide could not completely block the further binding of full-length amelogenin (data not shown), indicating that the segments other than the C-terminus are also involved in the amelogenin-crystal interactions. It has been suggested that the N-terminal region of amelogenin is able to bind to hydroxyapatite crystals to some degree[29]. Our present study suggests that the p.P70T mutation in amelogenin N-terminus increases the binding of amelogenin to apatite. It is possible that the replacement of proline with more flexible threonine makes the slightly buried N-terminus more prone to stretch out from the nanosphere structures, enhancing their chances to interact with the apatite. Therefore, we assume that the structure of amelogenin nanospheres is important for their binding affinity and ability to interact with the apatite crystals.

Extensive studies have shown that amelogenin nanospheres are directly involved in controlling the structural organization and growth habit of apatite crystals, and this control is affected by many factors, such as pH and the degree of ionic saturation[9,31]. To further identify the effect of the disturbed amelogenin self-assembly on the apatite growth, a dynamic titration was applied in our crystallization experiments. The dynamic titration allows for replenishment of the precipitating solutes by continuously supplying the solution with calcium, phosphate and hydroxyl ions. As such, this approach maintains the degree of saturation of the solution in the metastable range with regard to apatite, which facilitates a continuous and yet controlled crystal growth. Data from our dynamic settings showed that

p.P70T mutation of amelogenin induced severe retardation of the crystal growth as compared to control amelogenin. Aside from their function to support and protect the forming crystals, amelogenin nanospheres are also thought to create ionic channels through the apposition of their surfaces to facilitate ion transport for enamel biomineralization[32,33]. The packing pattern of the nanosphere structures and their individual size may affect the channeling[32]. Thus, the altered amelogenin nanospheres and their increased apatite-binding amount by p.P70T mutation may disrupt the optimal channeling conditions and thereby interfere with the flow of precursor ions, resulting in inhibited mineral growth.

In conclusion, the results of the present study strongly suggest that highly conserved Pro-70 of amelogenin may occupy a key position in the conformational transition and maintenance upon protein self-assembly. It may provide local rigidity and a specific turn in the nanosphere structures, which is essential for the interactions with neighboring molecules. Replacing this proline with much more flexible threonine disturbs the normal self-assembly and apatite binding behavior of the protein. These alterations further change the desired microenvironment for apatite crystal growth, leading to its retardation. The results presented in this study provide an important insight as to how p.P70T mutation causes AI. These and similar fundamental insights on the biological role of fine structural elements of protein ingredients of the enamel matrix may improve our knowledge of the process of amelogenesis and eventually help us imitate it *in vitro* with a higher precision and efficiency.

Acknowledgments

This research was supported byR01-DE015821, R01-DE17529 and R01-DE013508 from NIDCR.

REFERENCES

1. Aldred MJ, Savarirayan R, Crawford PJ. Amelogenesis imperfecta: a classification and catalogue for the 21st century. Oral Dis. 2003; 9:19–23. [PubMed: 12617253]
2. Simmer JP, Hu JC. Dental enamel formation and its impact on clinical dentistry. J Dent Educ. 2001; 65:896–905. [PubMed: 11569606]
3. Collier PM, Sauk JJ, Rosenbloom SJ, Yuan ZA, Gibson CW. An amelogenin gene defect associated with human X-linked amelogenesis imperfecta. Arch Oral Biol. 1997; 42:235–42. [PubMed: 9188994]
4. Hart PS, Aldred MJ, Crawford PJ, Wright NJ, Hart TC, Wright JT. Amelogenesis imperfecta phenotype-genotype correlations with two amelogenin gene mutations. Arch Oral Biol. 2002; 47:261–5. [PubMed: 11922869]
5. Ravassipour DB, Hart PS, Hart TC, Ritter AV, Yamauchi M, Gibson C, et al. Unique enamel phenotype associated with amelogenin gene (AMELX) codon 41 point mutation. J Dent Res. 2000; 79:1476–81. [PubMed: 11005731]
6. Li W, Gibson CW, Abrams WR, Andrews DW, DenBesten PK. Reduced hydrolysis of amelogenin may result in X-linked amelogenesis imperfecta. Matrix Biol. 2001; 19:755–60. [PubMed: 11223334]
7. Fincham AG, Moradian-Oldak J. Recent advances in amelogenin biochemistry. Connect Tissue Res. 1995; 32:119–24. [PubMed: 7554907]
8. Moradian-Oldak J, Simmer JP, Lau EC, Sarte PE, Slavkin HC, Fincham AG. Detection of monodisperse aggregates of a recombinant amelogenin by dynamic light scattering. Biopolymers. 1994; 34:1339–1347. [PubMed: 7948720]
9. Habelitz S, Denbesten PK, Marshall SJ, Marshall GW, Li W. Amelogenin control over apatite crystal growth is affected by the pH and degree of ionic saturation. Orthod Craniofac Res. 2005; 8:232–8. 2005. [PubMed: 16238603]

10. Moradian-Oldak J, Tan J, Fincham AG. Interaction of amelogenin with hydroxyapatite crystals: an adherence effect through amelogenin molecular self-association. Biopolymers. 1998; 46:225–238. [PubMed: 9715666]
11. Paine ML, Snead ML. Protein interactions during assembly of the enamel organic extracellular matrix. J Bone Miner Res. 1997; 12:221–227. [PubMed: 9041053]
12. Robinson C, Kirkham J, Briggs HD, Atkinson PJ. Enamel proteins: from secretion to maturation. J Dent Res. 1982; 16:1490–1495. [PubMed: 6958707]
13. Gibson CW, Yuan ZA, Hall B, Longenecker G, Chen E, Thyagarajan T, et al. Amelogenin-deficient mice display an amelogenesis imperfecta phenotype. J Biol Chem. 2001; 276:31871–5. [PubMed: 11406633]
14. Ellies LG, Nelson DG, Featherstone JD. Crystallographic structure and surface morphology of sintered carbonated apatites. J Biomed Mater Res. 1988; 22:541–53. [PubMed: 3410872]
15. Featherstone JD, Mayer I, Driessens FC, Verbeeck RM, Heijligers HJ. Synthetic apatites containing Na, Mg, and CO3 and their comparison with tooth enamel mineral. Calcif Tissue Int. 1983; 35:169–71. [PubMed: 6850399]
16. Tanimoto K, Le T, Zhu L, Chen J, Featherstone JD, Li W, et al. Effects of Fluoride on the Interactions between Amelogenin and Apatite Crystals. J Dent Res. 2008a; 87:39–44. [PubMed: 18096891]
17. DenBesten PK, Yan Y, Featherstone JD, Hilton JF, Smith CE, Li W. Effects of fluoride on rat dental enamel matrix proteinases. Arch Oral Biol. 2002; 47:763–70. [PubMed: 12446183]
18. Li W, Gao C, Yan Y, DenBesten P. X-linked amelogenesis imperfecta may result from decreased formation of tyrosine rich amelogenin peptide (TRAP). Arch Oral Bio. 2003; 48:177–83. [PubMed: 12648554]
19. Moisescu C, Jana C, Habelitz S, Carl G, Rüssel C. Oriented fluoroapatite glass-ceramics. J. Non-Cryst. Sol. 1999; 248:176–182.
20. Habelitz S, Kullar A, Marshall SJ, DenBesten PK, Balooch M, Marshall GW, et al. Amelogenin-guided crystal growth on fluoroapatite glass-ceramics. J Dent Res. 2004; 83:698–702. [PubMed: 15329375]
21. Habelitz S, DenBesten PK, Marshall SJ, Marshall GW, Li W. Self-assembly and effect on crystal growth of the leucine-rich amelogenin peptide. Eur J Oral Sci. 2006; 114(Suppl 1):315–9. discussion 327-9, 382. [PubMed: 16674705]
22. Habelitz S, Balooch M, Marshall S, Balooch G, Marshall G. In situ atomic force microscopy of partially demineralized human dentin collagen fibrils. J Struct Biol. 2002; 138:227–236. [PubMed: 12217661]
23. Uskokovic V, Kim MK, Li W, Habelitz S. Enzymatic Processing of Amelogenin during Continuous Crystallization of Apatite. J Mater Res. 2008; 23(12):3184–3195. [PubMed: 19177182]
24. Tanimoto K, Le T, Zhu L, Witkowska HE, Robinson S, Hall S, et al. Reduced amelogenin-MMP20 interactions in amelogenesis imperfecta. J Dent Res. 2008b; 87(5):451–5. [PubMed: 18434575]
25. Lakshminarayanan R, Fan D, Du C, Moradian-Oldak J. The role of secondary structure in the entropically driven amelogenin self-assembly. Biophys. J. 2007; 93:3664–3674. [PubMed: 17704165]
26. Moradian-Oldak J, Paine ML, Lei YP, Fincham AG, Snead ML. Self-assembly properties of recombinant engineered amelogenin proteins analyzed by dynamic light scattering and atomic force microscopy. J Struct Biol. 2000; 131(1):27–37. [PubMed: 10945967]
27. Creighton, TE. Proteins: Structures and Molecular Properties. Second Edition ed.. Freeman; New York: 1993.
28. Barth A, Zscherp C. What vibrations tell us about proteins. Q Rev Biophys. 2002; 35(4):369–430. [PubMed: 12621861]
29. Sire JY, Delgado S, Fromentin D, Girondot M. Amelogenin: lessons from evolution. Arch Oral Bio. 2005; 52:205–212. [PubMed: 15721151]
30. Vilhjalmsson B, Rasmussen A, Fabi B, van de Weert M, Hamelryck T, Lemoult S. Bioinformatic and experimental analysis of the secondary structure of amelogenin. European Cells and Materials. 2007; 14:104.

31. Iijima M, Moradian-Oldak J. Interactions of amelogenins with octacalcium phosphate crystal faces are dose dependent. Calcif Tissue Int. 2004; 74:522–531. [PubMed: 15354860]

32. Fincham AG, Moradian-Oldak J, Diekwisch TG, Lyaruu DM, Wright JT, Bringas P Jr, Slavkin HC. Evidence for amelogenin ‘nanospheres’ as functional components of secretory-stage enamel matrix. J Struct Biol. 1995; 115:50–59. [PubMed: 7577231]

33. Robinson C, Brookes SJ, Shore RC, Kirkham J. The developing enamel matrix: Nature and function. Eur Oral Sci. 1998; 106:282–291.

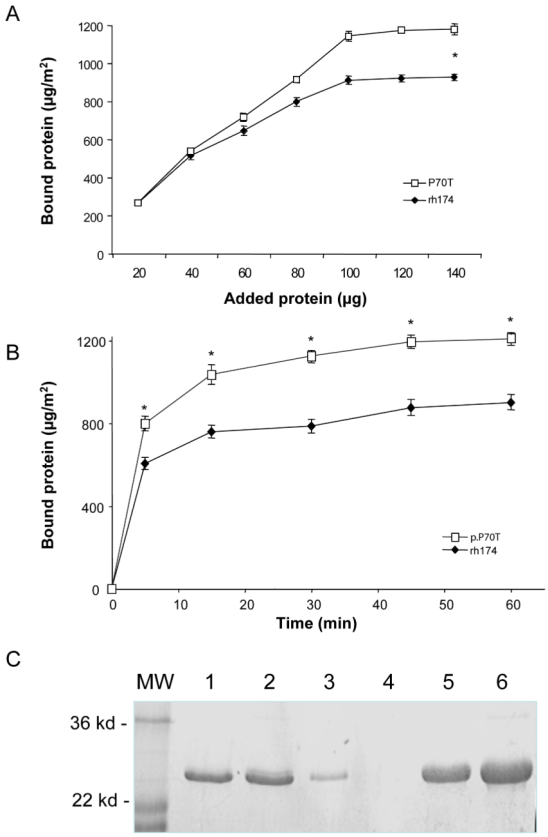

Fig. 1. Comparisons of apatite bindings of rh174 and p.P70T amelogenins by protein assay and SDS-PAGE

(A) The saturated amounts of rh174 amelogenin and p.P70T mutant bound to HAP were 875.155 ± 37.083 and 1194.067 ± 32.328 $\mu g/m^2$ respectively, showing a significant difference in apatite binding between these two types of amelogenins (*$P < 0.01$). (B) Time curves of adsorption of rh174 amelogenin and p.P70T mutant to CHAP. More than 75% of both rh174 and p.P70T amelogenins bound to CHAP in initial 5 minutes of the binding reactions. The bindings of these amelogenins to CHAP reached their plateaus after 15 minutes of incubation. The binding amounts showed significant differences (*$P<0.01$) at all time points after 5-minute incubation. (C) The SDS-PAGE revealed that more p.P70T mutated amelogenin was bound to HAP, leaving less protein in the supernatants. Lane 1, rh174 amelogenin control without CHAP; Lane 2, p.P70T mutated amelogenin control without CHAP; Lane 3, rh174 amelogenin remained in supernatant after binding; Lane 4, p.P70Tmutated amelogenin remained in supernatant after binding; Lane 5, rh174 amelogenin bound on CHAP; Lane 6, p.P70Tmutated amelogenin bound on CHAP.

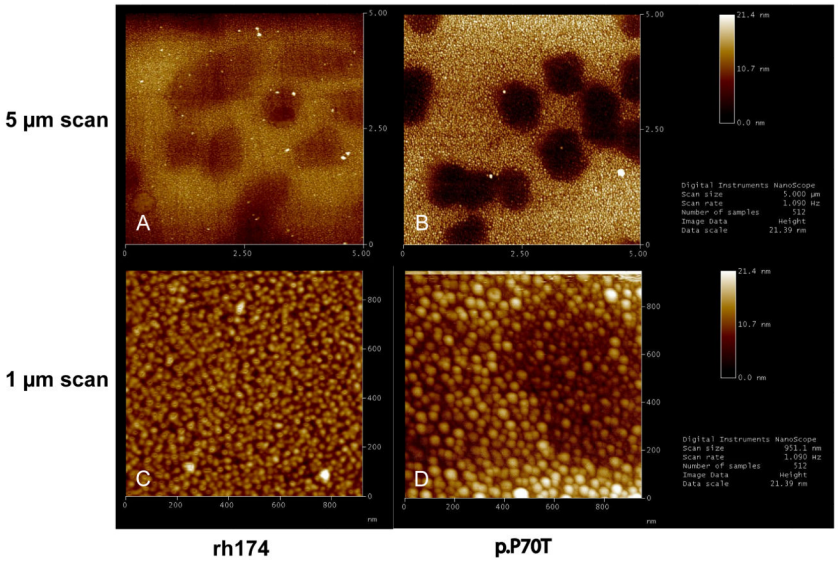

Fig.2. AFM comparisons of rh174 and p.P70T amelogenin assemblies on apatite crystal surface

Both rh174 and p.P70T assemblies were able to bind to the surfaces of glass (darker area) and FAP crystals (lighter area) at their (001) faces (3A and 3B). p.P70T mutant formed larger and more heterogeneous nanosphere assemblies (B and D) than rh174 (A and C).

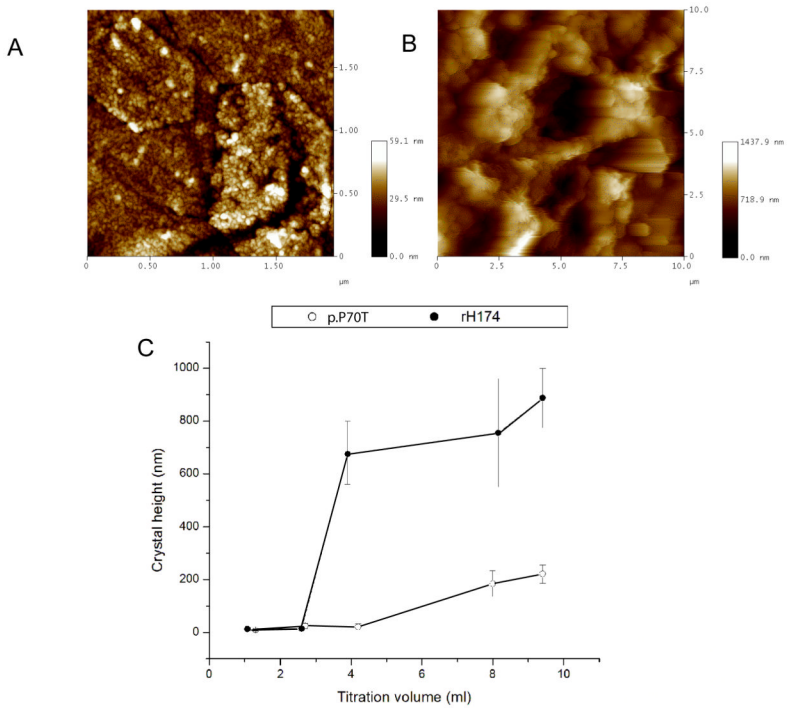

Fig.3. AFM imaging of apatite crystals grown in the presence of rh174 and p.P70T amelogenins

AFM image of FAP crystals sampled out after 4.2 ml of titration volume in a dynamic precipitation experiment utilizing p.P70T (A) and rh174 (B), and a comparison of the height of substrate FAP crystals grown after different reaction times from suspensions comprising rh174 and p.P70T (C).